PERGAMON

International Journal of Solids and Structures 37 (2000) 1103–1117

INTERNATIONAL JOURNAL OF SOLIDS and STRUCTURES

www.elsevier.com/locate/ijsolstr

Exact and approximate dynamic analysis of circular arches using DQM

M.A. De Rosa*, C. Franciosi

Department of Structural Engineering, University of Basilicata, Potenza, Italy

Received 20 September 1997; in revised form 1 September 1998

Abstract

A modified version of the differential quadrature method is applied to two versions of the sixth-order differential equation of motion governing free in-plane inextensional vibrations of circular arches (see Henrych, 1981).

All the boundary conditions can be imposed exactly, without introducing δ points (see e.g. Bert and Malik, 1996). Consequently, the results are calculated with high precision, and a comparison between exact and approximate frequencies becomes possible.

The convergence rate of the discretization method is shown to be very fast, even for the higher eigenvalues, so that a small number of Lagrangian coordinates permits a good approximation to the true results. It is shown that the approximate formulation leads to noticeable errors for the first frequencies of deep arches, whereas shallow arches and higher-order frequencies can be safely calculated with the simplified approach.

The paper ends with some tables in which the first ten free vibrations frequencies for clamped arches, two-hinged arches and cantilever arches are compared with some known results from the literature.

1. Introduction

Let us consider the circular arch in Fig. 1, with radius R, opening angle θ_0, Young's modulus E, cross-sectional area, A, moment of inertia I and distributed mass μ.

The dynamic analysis of this structure, in the presence of shear deformation and rotary inertia, leads to complicated governing equations, especially if the arch axis is considered to be extensible.

On the other hand, the effects of shear deformation and rotary inertia can be safely neglected, if the arch is considered to be thin, and in this case the equation of motion can be expressed as (cf Henrych, 1981):

* Corresponding author: Department of Structural Engineering, Faculty of Engineering, University of Basilicata, Via della Tecnica 3, 85100, Potenza, Italy. Fax: +0039-971-57477.

0020-7683/00/$ - see front matter
PII: S0020-7683(98)00275-3

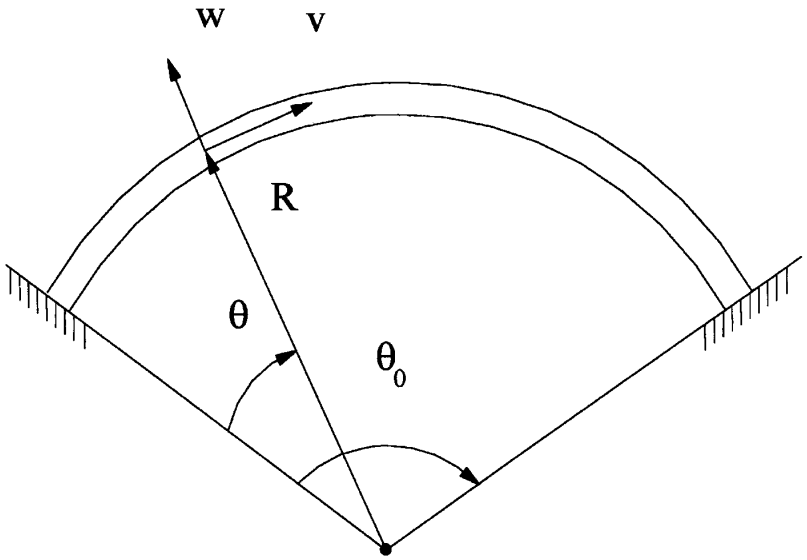

Fig. 1. The structural system under investigation.

$$\frac{\partial^6 v}{\partial\theta^6}+2\frac{\partial^4 v}{\partial\theta^4}+\frac{\partial^2 v}{\partial\theta^2}+\frac{\mu R^4}{EI}\left[\left(1-\frac{I}{AR^2}\right)\frac{\partial^4 v}{\partial\theta^2\,\partial t^2}-\frac{\partial^2 v}{\partial t^2}-\frac{I}{AR^2}\frac{\partial^6 v}{\partial\theta^4\,\partial t^2}\right]-\frac{\mu^2 R^6}{E^2 IA}\frac{\partial^4 v}{\partial t^4}=0 \tag{1}$$

where $v = v(\theta, t)$, and with a similar equation for the other displacement component.

Moreover, if the arch axis is considered to be inextensible, the previous equation becomes:

$$\frac{\partial^6 v}{\partial\theta^6}+2\frac{\partial^4 v}{\partial\theta^4}+\frac{\partial^2 v}{\partial\theta^2}+\frac{\mu R^4}{EI}\left[\frac{\partial^4 v}{\partial\theta^2\,\partial t^2}-\frac{\partial^2 v}{\partial t^2}\right]=0 \tag{2}$$

Finally, another simplifying assumption can be introduced by neglecting the tangential inertial forces expressed by the last term of the previous equation:

$$\frac{\partial^6 v}{\partial\theta^6}+2\frac{\partial^4 v}{\partial\theta^4}+\frac{\partial^2 v}{\partial\theta^2}+\frac{\mu R^4}{EI}\frac{\partial^4 v}{\partial\theta^2\,\partial t^2}=0 \tag{3}$$

It is intuitively clear that the above introduced hypothesis is reasonable for shallow arches, whereas for steep arches it can lead to significant errors. Some numerical results reported in Henrych (1981), p. 186, confirm this statement.

In the following, the attention will be restricted to eqn (2) (henceforth 'exact equation') and eqn (3) (henceforth 'approximate equation').

Quite recently (see Kang et al., 1996), eqn (2) has been solved by using the differential quadrature method (henceforth DQM), and some preliminary results have been given for clamped arches and simply supported arches. The analysis was restricted to the fundamental frequency, and, moreover, the boundary conditions were imposed by using the approximate double δ method.

More recently, a new procedure was proposed for fourth-order equations by Wang et al. (1993) and by Chen et al. (1997), which allow the exact satisfaction of all the four boundary conditions, and a

straight-forward generalization was proposed for the same systems (see De Rosa and Franciosi, 1998a), even in the presence of nonclassical boundary conditions (De Rosa and Franciosi, 1998b).

In this paper the above-mentioned approach is extended to sixth-order equations, so enabling the analysis of arbitrary boundary conditions and the calculation of the higher frequencies. Clamped arches, double-hinged arches and cantilever arches are treated in detail, but the procedure remains valid for other kinds of constraints, and the first ten frequencies are calculated for various opening angles.

The numerical results are compared with two different exact approaches, developed by Henrych (1981) and Wassermann (1997), and with some other numerical methods such as finite elements and cell discretization method (see Auciello and De Rosa, 1984).

It will be seen that the results are quite satisfactory, even for very deep arches, so confirming the efficiency of DQM in comparison with other numerical techniques.

2. The structural system

The boundary conditions which will be considered in the following are expressed by:

$$\text{A. Clamped end} \quad \rightarrow v = \frac{\partial v}{\partial \theta} = \frac{\partial^2 v}{\partial \theta^2} = 0$$

$$\text{B. Supported end} \quad \rightarrow v = \frac{\partial v}{\partial \theta} = \frac{\partial^3 v}{\partial \theta^3} = 0$$

$$\text{C. Free end} \quad \rightarrow M = T = N = 0 \tag{4}$$

where M, T and N are the bending moment, the shear force and the normal force, respectively, and can be expressed as:

$$M(\theta, t) = -\frac{EI}{R^2}\left[\frac{\partial^3 v(\theta, t)}{\partial \theta^3} + \frac{\partial v(\theta, t)}{\partial \theta}\right]$$

$$T(\theta, t) = -\frac{EI}{R^3}\left[\frac{\partial^4 v(\theta, t)}{\partial \theta^4} + \frac{\partial^2 v(\theta, t)}{\partial \theta^2}\right]$$

$$N(\theta, t) = \frac{EI}{R^3}\left[\frac{\partial^5 v(\theta, t)}{\partial \theta^5} + \frac{\partial^3 v(\theta, t)}{\partial \theta^3}\right] + R\mu\frac{\partial^3 v(\theta, t)}{\partial \theta\, \partial t^2} \tag{5}$$

By assuming a solution of the form:

$$v(\theta, t) = v(\theta) f(t) \tag{6}$$

with $f(t)$ harmonic function with frequency ω, the exact differential equation of motion becomes:

$$\frac{\partial^6 v(\theta)}{\partial \theta^6} + 2\frac{\partial^4 v(\theta)}{\partial \theta^4} + \frac{\partial^2 v(\theta)}{\partial \theta^2} = \frac{\mu R^4 \omega^2}{EI}\left[\frac{\partial^2 v(\theta)}{\partial \theta^2} - v(\theta)\right] \tag{7}$$

with a similar expression for the approximate equation.

It is now convenient to map the physical domain $[0, \theta_0]$ onto the natural Gaussian domain $[-1, 1]$, by

means of the transformation:

$$\xi(\theta) = 2\left(\frac{\theta}{\theta_0}\right) - 1 \tag{8}$$

where ξ is called the natural coordinate.

It follows that the differential eqn (7) becomes:

$$\frac{64}{\theta_0^6}\frac{\partial^6 v(\xi)}{\partial \xi^6} + \frac{32}{\theta_0^4}\frac{\partial^4 v(\xi)}{\partial \xi^4} + \frac{4}{\theta_0^2}\frac{\partial^2 v(\xi)}{\partial \xi^2} = \Omega^2\left(\frac{4}{\theta_0^2}\frac{\partial^2 v(\xi)}{\partial \xi^2} - v(\xi)\right) \tag{9}$$

where:

$$\Omega^2 = \frac{\mu\omega^2 R^4}{EI} \tag{10}$$

is the nondimensional frequency.

It is possible to define the couple of differential operators:

$$\mathscr{L} = \frac{64}{\theta_0^6}\frac{\partial^6}{\partial \xi^6} + \frac{32}{\theta_0^4}\frac{\partial^4}{\partial \xi^4} + \frac{4}{\theta_0^2}\frac{\partial^2}{\partial \xi^2} \tag{11}$$

and:

$$\mathscr{M} = \frac{4}{\theta_0^2}\frac{\partial^2}{\partial \xi^2} - \mathscr{I} \tag{12}$$

where $\mathscr{I}$ is the identity operator.

Finally, the boundary value problem can be expressed as:

$$\mathscr{L}v = \Omega^2 \mathscr{M} v \tag{13}$$

with the appropriate six boundary conditions.

3. The discretization method

According to the DQM, the first step toward the numerical solution of the above derived boundary value problem is to divide the natural interval into n segments defined by means of $n+1$ points located at the abscissae $\xi_1, \xi_2, \ldots, \xi_{n+1}$.

Then, the following set of $(n+11)$ nodal unknowns is defined:

$$\mathbf{d}^{\mathrm{T}} = \left\{v_1, v_1', v_1'', v_1''', v_1'''', v_1''''', v_2, \ldots, v_{n+1}', v_{n+1}'', v_{n+1}''', v_{n+1}'''', v_{n+1}'''''\right\} \tag{14}$$

and the displacement $v(\xi)$ of the beam is approximated as:

$$v(\xi) = \boldsymbol{\alpha}\mathbf{C} = \sum_{i=1}^{n+11} \alpha_i C_i \tag{15}$$

where $\boldsymbol{\alpha}$ is a row vector of monomials, and $\mathbf{C}$ is a column vector of Lagrangian coordinates.

Two choices of monomials arise quite naturally from the discretization procedure, i.e. $\alpha_i = \xi^{i-1}$ and $\alpha_i = T_{i-1}(\xi)$, where $T_i(\xi)$ is the Chebyshev polynomials of the first kind (see Bert and Malik, 1996).

In the first case the sampling points are uniformly distributed along the natural interval:

$$\xi_i = \frac{2(i-1)-n}{n}; \quad i = 1, 2, \ldots, n+1 \tag{16}$$

In the second case the sampling points will be conveniently located at the so-called Gauss–Lobatto–Chebyshev points:

$$\xi_i = -\cos\left(\frac{\pi(i-1)}{n}\right); \quad i = 1, 2, \ldots, n+1 \tag{17}$$

From eqn (15) it is easily seen that:

$$v^{(i)}(\xi) = \boldsymbol{\alpha}^{(i)}\mathbf{C}; \quad i = 1, \ldots, 5 \tag{18}$$

and therefore:

$$\mathbf{d} = \left\{ \begin{array}{c} \boldsymbol{\alpha}_1 \\ \boldsymbol{\alpha}_1' \\ \boldsymbol{\alpha}_1'' \\ \boldsymbol{\alpha}_1''' \\ \boldsymbol{\alpha}_1'''' \\ \boldsymbol{\alpha}_1''''' \\ \boldsymbol{\alpha}_2 \\ \vdots \\ \boldsymbol{\alpha}_{n+1} \\ \boldsymbol{\alpha}_{n+1}' \\ \boldsymbol{\alpha}_{n+1}'' \\ \boldsymbol{\alpha}_{n+1}''' \\ \boldsymbol{\alpha}_{n+1}'''' \\ \boldsymbol{\alpha}_{n+1}''''' \end{array} \right\} \mathbf{C} = \mathbf{N}_0\mathbf{C} \tag{19}$$

Following the same approach as in Chen et al. (1997), we define the weighting coefficients of the first sixth derivatives, as follows:

$$\begin{aligned} &\mathbf{A} = \mathbf{N}_0'\mathbf{N}_0^{-1}; \quad \mathbf{B} = \mathbf{AA}; \quad \mathbf{C} = \mathbf{AAA} \\ &\mathbf{D} = \mathbf{AAAA}; \quad \mathbf{E} = \mathbf{AAAAA}; \quad \mathbf{F} = \mathbf{AAAAAA} \end{aligned} \tag{20}$$

This discretized version of eqn (13) is given by:

$$\begin{bmatrix} L_{1,1} & L_{1,2} & \dots & L_{1,n+11} \\ L_{2,1} & L_{2,2} & \dots & L_{2,n+11} \\ L_{3,1} & L_{3,2} & \dots & L_{3,n+11} \\ L_{4,1} & L_{4,2} & \dots & L_{4,n+11} \\ L_{5,1} & L_{5,2} & \dots & L_{5,n+11} \\ L_{6,1} & L_{6,2} & \dots & L_{6,n+11} \\ L_{7,1} & L_{7,2} & \dots & L_{7,n+11} \\ \vdots & \vdots & \ddots & \vdots \\ L_{n+11,1} & L_{n+11,2} & \dots & L_{n+11,n+11} \end{bmatrix} \begin{bmatrix} \upsilon_1 \\ \upsilon_1' \\ \upsilon_1'' \\ \upsilon_1''' \\ \upsilon_1'''' \\ \upsilon_1''''' \\ \upsilon_2 \\ \vdots \\ \upsilon_{n+1}''''' \end{bmatrix}$$

$$= \Omega^2 \begin{bmatrix} M_{1,1} & M_{1,2} & \dots & M_{1,n+11} \\ M_{2,1} & M_{2,2} & \dots & M_{2,n+11} \\ M_{3,1} & M_{3,2} & \dots & M_{3,n+11} \\ M_{4,1} & M_{4,2} & \dots & M_{4,n+11} \\ M_{5,1} & M_{5,2} & \dots & M_{5,n+11} \\ M_{6,1} & M_{6,2} & \dots & M_{6,n+11} \\ M_{7,1} & M_{7,2} & \dots & M_{7,n+11} \\ \vdots & \vdots & \ddots & \vdots \\ M_{n+11,1} & M_{n+11,2} & \dots & M_{n+11,n+11} \end{bmatrix} \begin{bmatrix} \upsilon_1 \\ \upsilon_1' \\ \upsilon_1'' \\ \upsilon_1''' \\ \upsilon_1'''' \\ \upsilon_1''''' \\ \upsilon_2 \\ \vdots \\ \upsilon_{n+1}''''' \end{bmatrix} \tag{21}$$

where the matrices **L** and **M** are the discretized version of the differential operators $\mathscr{L}$ and $\mathscr{M}$:

$$L_{ij} = \frac{64}{\theta_0^6} F_{ij} + \frac{32}{\theta_0^4} D_{ij} + \frac{4}{\theta_0^2} B_{ij} \quad i,j = 1,2,\dots,n+11 \tag{22}$$

$$M_{ij} = \frac{4}{\theta_0^2} B_{ij} - \delta_{ij} \quad i,j = 1,2,\dots,n+11 \tag{23}$$

where δ_{ij} is the well-known Kronecker operator, and should be neglected if the approximate solution has to be used.

4. The boundary conditions

Let us consider first the clamped arch, for which the six boundary conditions are expressed as:

$$\upsilon(-1) = \left.\frac{\partial \upsilon}{\partial \theta}\right|_{\theta=-1} = \left.\frac{\partial^2 \upsilon}{\partial \theta^2}\right|_{\theta=-1} = 0$$

$$\upsilon(1) = \left.\frac{\partial \upsilon}{\partial \theta}\right|_{\theta=1} = \left.\frac{\partial^2 \upsilon}{\partial \theta^2}\right|_{\theta=1} = 0 \tag{24}$$

In order to impose these conditions, it is convenient to interchange the rows (and columns) $(n+6)$, $(n+7)$ and $(n+8)$ of the matrices **L** and **M** with the fourth, fifth and sixth rows (and columns), so that it is possible to write:

$$\begin{pmatrix} \mathbf{L}_{pp} & \mathbf{L}_{pa} \\ \mathbf{L}_{ap} & \mathbf{L}_{aa} \end{pmatrix} \begin{pmatrix} \mathbf{v}_p \\ \mathbf{v}_a \end{pmatrix} = \Omega^2 \begin{pmatrix} \mathbf{M}_{pp} & \mathbf{M}_{pa} \\ \mathbf{M}_{ap} & \mathbf{M}_{aa} \end{pmatrix} \begin{pmatrix} \mathbf{v}_p \\ \mathbf{v}_a \end{pmatrix} \tag{25}$$

where $\mathbf{v}_p$ is the vector of the passive coordinates:

$$\mathbf{v}_p^T = \left(\upsilon_1 \;\; \upsilon_1' \;\; \upsilon_1'' \;\; \upsilon_{n+1} \;\; \upsilon_{n+1}' \;\; \upsilon_{n+1}''\right) \tag{26}$$

and $\mathbf{v}_a$ is the vector of the active coordinates:

$$\mathbf{v}_a^T = \left(\upsilon_2 \;\; \upsilon_3 \;\; \ldots \;\; \upsilon_1''' \;\; \upsilon_1'''' \;\; \upsilon_1''''' \;\; \upsilon_{n+1}''' \;\; \upsilon_{n+1}'''' \;\; \upsilon_{n+1}'''''\right) \tag{27}$$

It is easy to realize that the modified system:

$$\begin{pmatrix} \mathbf{I} & \mathbf{0} \\ \mathbf{L}_{ap} & \mathbf{L}_{aa} \end{pmatrix} \begin{pmatrix} \mathbf{v}_p \\ \mathbf{v}_a \end{pmatrix} = \Omega^2 \begin{pmatrix} \mathbf{0} & \mathbf{0} \\ \mathbf{M}_{ap} & \mathbf{M}_{aa} \end{pmatrix} \begin{pmatrix} \mathbf{0} \\ \mathbf{v}_a \end{pmatrix} \tag{28}$$

satisfies exactly all the boundary conditions:

Moreover, the above derived system can be solved very easily, because it suffices to calculate the eigenvalues of the reduced system:

$$\mathbf{L}_{aa}\mathbf{v}_p = \Omega^2 \mathbf{M}_{aa}\mathbf{v}_a \tag{29}$$

The hinged-hinged arch is defined by the boundary conditions:

$$\upsilon(-1) = \left.\frac{\partial \upsilon}{\partial \theta}\right|_{\theta=-1} = \left.\frac{\partial^3 \upsilon}{\partial \theta^3}\right|_{\theta=-1} = 0$$

$$\upsilon(1) = \left.\frac{\partial \upsilon}{\partial \theta}\right|_{\theta=1} = \left.\frac{\partial^3 \upsilon}{\partial \theta^3}\right|_{\theta=1} = 0 \tag{30}$$

and can be treated quite similarly to the clamped case.

In fact, the passive coordinates are now given by:

$$\mathbf{v}_p^T = \left(\upsilon_1 \;\; \upsilon_1' \;\; \upsilon_{n+1} \;\; \upsilon_1''' \;\; \upsilon_{n+1}' \;\; \upsilon_{n+1}'''\right) \tag{31}$$

whereas the vector of the active coordinates is equal to:

$$\mathbf{v}_a^T = \left(\upsilon_2 \;\; \upsilon_3 \;\; \ldots \;\; \upsilon_1'' \;\; \upsilon_1'''' \;\; \upsilon_{n+1}'' \;\; \upsilon_1''''' \;\; \upsilon_{n+1}'''' \;\; \upsilon_{n+1}'''''\right) \tag{32}$$

Therefore, the rows (and columns) $(n+6)$, $(n+7)$ and $(n+9)$ of the matrices $\mathbf{L}$ and $\mathbf{M}$ should be interchanged with the third, fifth and sixth rows (and columns).

Even in this case it suffices to solve the reduced system (29) of order $n + 5$.

The cantilever arch poses some additional problem, due to the presence of the eigenvalue in the boundary conditions. Actually, the clamped-free arch is defined by [see eqn (5)]:

$$\upsilon(-1) = \left.\frac{\partial \upsilon}{\partial \theta}\right|_{\theta=-1} = \left.\frac{\partial^2 \upsilon}{\partial \theta^2}\right|_{\theta=-1} = 0 \tag{33}$$

$$\left.\frac{\partial \upsilon}{\partial \theta}\right|_{\theta=1} + \frac{4}{\theta_0^2}\left.\frac{\partial^3 \upsilon}{\partial \theta^3}\right|_{\theta=1} = 0; \quad \left.\frac{\partial^2 \upsilon}{\partial \theta^2}\right|_{\theta=1} + \frac{4}{\theta_0^2}\left.\frac{\partial^4 \upsilon}{\partial \theta^4}\right|_{\theta=1} = 0; \tag{34}$$

$$\left.\frac{\partial^5 \upsilon}{\partial \theta^5}\right|_{\theta=1}+\frac{\theta_0^2}{4}\left.\frac{\partial^3 \upsilon}{\partial \theta^3}\right|_{\theta=1}-\Omega^2\frac{\theta_0^4}{16}\left.\frac{\partial \upsilon}{\partial \theta}\right|_{\theta=1}=0 \tag{35}$$

so that it seems convenient to choose the following passive coordinates:

$$\mathbf{v}_{\mathrm{p}}^{\mathrm{T}}=\left(\upsilon_1\ \upsilon_1'\ \upsilon_1''\ \upsilon_{n+1}'\ \upsilon_{n+1}''\ \upsilon_{n+1}''''\right) \tag{36}$$

and consequently:

$$\mathbf{v}_{\mathrm{a}}^{\mathrm{T}}=\left(\upsilon_2\ \upsilon_3\ \ldots\ \upsilon_{n+1}\ \upsilon_1'''\ \upsilon_1''''\ \upsilon_{n+1}'''\ \upsilon_{n+1}''''\ \upsilon_1''''\right) \tag{37}$$

Rows (and columns) $(n+7)$, $(n+8)$ and $(n+11)$ of the matrices $\mathbf{L}$ and $\mathbf{M}$ should be interchanged with the fourth, fifth and sixth rows (and columns). In addition, (see eqn (25)) matrix $\mathbf{L}_{\mathrm{pp}}$ will be given by the identity matrix, as before, but matrix $\mathbf{L}_{\mathrm{pa}}$ will contain the nonzero terms:

$$\mathbf{L}_{\mathrm{pa}}(4,n+9)=\frac{4}{\theta_0^2};\quad \mathbf{L}_{\mathrm{pa}}(5,n+10)=\frac{4}{\theta_0^2};\quad \mathbf{L}_{\mathrm{pa}}(6,n+9)=\frac{\theta_0^2}{4} \tag{38}$$

and the matrix $\mathbf{M}_{\mathrm{pp}}$ will contain the single nonzero term:

$$\mathbf{M}_{\mathrm{pp}}(6,4)=\frac{\theta_0^4}{16} \tag{39}$$

The simplest way to solve the resulting system seems to invert the complete $(n+11, n+11)$ $\mathbf{L}$ matrix and to find the eigenvalues of the matrix $\mathbf{L}^{-1}\mathbf{M}$. After disregarding the zero eigenvalues, the frequencies can be found as the inverse of the eigenvalues.

5. Numerical results

A small *Mathematica* notebook was written (see Wolfram, 1991), following closely the above developed theory. All the numerical approximations were ruled out until the eigenvalues calculations, so minimizing the potential source of numerical instabilities.

Table 1
Convergence study for a cantilever circular arch with opening angle $\theta_0 = 180°$. Exact theory

Ω^2	$n=5$	$n=10$	$n=15$	$n=20$
Ω_1^2	0.4351587	0.4351653	0.4351653	0.4351653
Ω_2^2	1.3749781	1.3749865	1.3749865	1.3749865
Ω_3^2	4.7085858	4.7090534	4.7090534	4.7090534
Ω_4^2	10.459782	10.515076	10.515099	10.515099
Ω_5^2		18.391839	18.392165	18.392166
Ω_6^2		28.374614	28.334995	28.335013
Ω_7^2		40.456956	40.292906	40.292191
Ω_8^2		52.153273	54.278495	54.266250
Ω_9^2			70.102498	70.245294
Ω_{10}^2			87.397703	88.210740

Table 2
Shallow clamped arches. Approximate theory

Ω^2	$\theta_0=20°$		$\theta_0=40°$		$\theta_0=80°$	
	Henrych	DQM	Henrych	DQM	Henrych	DQM
Ω_1^2	505.404	505.404	125.792	125.792	30.894	30.894
Ω_2^2	910.100	910.100	226.910	226.910	56.114	56.114
Ω_3^2	1639.391	1639.391	409.204	409.204	101.658	101.658
Ω_4^2	2374.823	2374.823	593.043	593.043	147.598	147.598
Ω_5^2	3421.348	3421.348	854.661	854.661	219.989	219.989
Ω_6^2	4483.458	4483.458	1120.178	1120.178	279.358	279.358
Ω_7^2	5851.325	5851.321	1462.137	1462.136	364.841	364.840
Ω_8^2	7238.872	7239.000	1809.018	1809.050	451.555	451.563
Ω_9^2	8929.311	8931.596	2231.623	2232.194	557.201	557.344
Ω_{10}^2	10,641.755	10,616.440	2659.730	2653.402	664.224	662.642

Table 3
Deep clamped arches. Approximate theory

Ω^2	$\theta_0=120°$		$\theta_0=160°$		$\theta_0=180°$
	Henrych	DQM	Henrych	DQM	DQM
Ω_1^2	13.328	13.3281	7.190	7.18982	5.53832
Ω_2^2	24.488	24.4888	13.423	13.4234	10.4393
Ω_3^2	44.707	44.7068	24.775	24.7755	19.3980
Ω_4^2	65.109	65.1089	36.239	36.2388	28.4488
Ω_5^2	94.161	94.1614	52.572	52.5723	41.3501
Ω_6^2	123.651	123.651	69.154	69.1543	54.4489
Ω_7^2	161.638	161.638	90.517	90.517	71.3258
Ω_8^2	200.173	200.177	112.189	112.191	88.4496
Ω_9^2	247.123	247.187	138.596	138.632	109.339
Ω_{10}^2	294.686	293.983	165.348	164.952	130.135

In order to check the exactness of the proposed approach, and the convergence rate of the method, let us consider a cantilever arch with opening angle $\theta_0 = \pi$. In Table 1 the first nondimensional frequencies are reported, using the monomials $\alpha_i = \xi^{i-1}$ and four different discretization levels. In the first column the arch was divided into $n = 5$ segments, identified by $n + 1 = 6$ equally spaced points. Consequently, an eigenvalue problem of order $n + 11 = 16$ has been solved. In the other columns, the arch has been divided into 10, 15 and 20 segments, respectively.

As can be seen, the first three frequencies are well approximated even for the coarse discretization,

Table 4
Shallow clamped arches. Exact theory

Ω^2	$\theta_0 = 20°$		$\theta_0 = 40°$		$\theta_0 = 180°$	
	Henrych	DQM	Henrych	DQM	Henrych	DQM
Ω_1^2	504.71254	503.54975	125.13412	123.97643	30.35434	29.21752
Ω_2^2	910.35841	909.14513	227.17462	225.96257	56.40168	55.19468
Ω_3^2	1638.49717	1637.2585	408.34864	407.11089	100.93967	99.70548
Ω_4^2	2375.04899	2373.7926	593.27251	592.01656	147.84397	146.58936
Ω_5^2	3420.37593	3419.10786	853.73153	852.46392	212.21124	210.94480
Ω_6^2		4482.39181		1119.11574		278.31116
Ω_7^2		5849.02420		1459.88596		362.75072
Ω_8^2		7237.91268		1807.96683		450.49406
Ω_9^2		8929.26520		2229.91209		555.22808
Ω_{10}^2		10,615.3320		2652.29756		661.55269

Table 5
Deep clamped arches. Exact theory

Ω^2	$\theta_0 = 120°$		$\theta_0 = 160°$		$\theta_0 = 180°$	
	Henrych	DQM	Henrych	DQM	Archer	DQM
Ω_1^2	12.94860	11.84758	6.97826	5.927444	4.3841	4.384430
Ω_2^2	24.81030	23.61261	13.78714	12.60396		9.651897
Ω_3^2	44.16960	42.94082	24.42701	23.20534		17.92179
Ω_4^2	65.38026	64.12795	36.54238	35.29352		27.52389
Ω_5^2	93.57901	92.31426	52.18717	50.92456		39.79536
Ω_6^2		122.62793		68.16142		53.47322
Ω_7^2		159.75261		88.83522		69.73749
Ω_8^2		199.13032		111.17408		87.44824
Ω_9^2		245.28043		136.93164		107.73308
Ω_{10}^2		292.91630		163.91439		129.11257

and the first five frequencies remain unchanged for the two finest discretization levels. In the following, all the examples will be given for $n = 20$, even because the computational effort is negligible.

In Tables 2–5 the clamped arches are examined. More precisely, Tables 2 and 3 refer to the approximate theory, whereas Tables 4 and 5 contain the frequencies as given by the exact theory. It is worth noting that the difference between these two approaches reduces to neglect the identity operator in eqn (12), or, equivalently, the Kronecker delta in eqn (23).

The first ten nondimensional free vibration frequencies were calculated for six different opening

Table 6
Shallow two-hinged arches. Approximate theory

Ω^2	$\theta_0 = 20°$		$\theta_0 = 40°$		$\theta_0 = 80°$	
	Henrych	DQM	Henrych	DQM	Henrych	DQM
Ω_1^2	323.000	323.000	80.000	80.000	19.250	19.250
Ω_2^2	690.898	690.898	172.005	172.005	42.283	42.283
Ω_3^2	1295.000	1295.000	323.000	323.000	80.000	180.000
Ω_4^2	1988.835	1988.835	496.470	496.470	123.379	123.379
Ω_5^2	2915.000	2915.000	728.000	728.000	181.250	181.250
Ω_6^2	3933.560	3933.559	982.646	982.646	244.917	244.917
Ω_7^2	5183.000	5182.980	1295.000	1294.995	323.000	322.999
Ω_8^2	6525.941	6526.645	1630.739	1630.915	406.938	406.982
Ω_9^2	8099.000	8106.193	2024.000	2025.799	505.250	505.700
Ω_{10}^2	9766.176	9685.260	2440.797	2420.5627	609.452	604.388

Table 7
Deep two-hinged arches. Approximate theory

Ω^2	$\theta_0 = 120°$		$\theta_0 = 160°$		$\theta_0 = 180°$
	Henrych	DQM	Henrych	DQM	DQM
Ω_1^2	8.000	8.000	4.063	4.063	3.000
Ω_2^2	18.261	18.261	9.855	9.855	7.588
Ω_3^2	35.000	35.000	19.250	19.250	15.000
Ω_4^2	54.288	54.288	30.107	30.107	23.582
Ω_5^2	80.000	80.000	44.563	44.563	35.000
Ω_6^2	108.301	108.301	60.485	60.485	47.583
Ω_7^2	143.000	142.999	80.000	80.000	63.000
Ω_8^2	180.309	180.328	100.988	100.999	79.593
Ω_9^2	224.000	224.200	125.563	125.676	99.090
Ω_{10}^2	270.314	268.060	151.615	150.345	118.580

angles, from $\theta_0 = 20°$ to $\theta_0 = 180°$, and the results are compared, wherever possible, with the eigenvalues reported by Henrych (1981).

It is possible to draw the following conclusions:

- for the approximate theory, the discrepancies between the Henrych values and the DQM results are negligible, even for the higher frequencies;
- for the exact theory, the agreement is less satisfactory. We suspect that the numerical approximate procedure used in Henrych (1981), p. 185 was not precise enough in calculating the roots of the

Table 8
Shallow two-hinged arches. Exact theory

Ω^2	$\theta_0 = 20°$		$\theta_0 = 40°$		$\theta_0 = 80°$	
	Henrych	DQM	Henrych	DQM	Henrych	DQM
Ω_1^2	322.84610	321.51482	79.88299	78.55804	19.26240	17.96407
Ω_2^2	691.34784	690.04207	172.46258	171.15800	42.76714	41.46761
Ω_3^2	1294.84289	1293.51005	322.87042	321.53908	79.96697	78.64105
Ω_4^2	1989.30118	1987.97806	496.94001	495.61730	123.86315	122.54186
Ω_5^2	2914.84270	2913.50952	727.86936	726.53690	181.21200	179.88186
Ω_6^2		3932.70542		981.79510		244.0783
Ω_7^2		5181.48967		1293.5317		321.6289
Ω_8^2		6525.79373		1630.0663		406.1437
Ω_9^2		8104.68636		2024.3199		504.3162
Ω_{10}^2		9684.45635		2419.7613		603.5950

Table 9
Deep two-hinged arches. Exact theory

Ω^2	$\theta_0 = 120°$		$\theta_0 = 160°$		$\theta_0 = 180°$	
	Henrych	DQM	Henrych	DQM	Wasserman	DQM
Ω_1^2	8.17865	6.92676	4.27735	3.21790	2.267	2.26674
Ω_2^2	18.78599	17.49631	10.42841	9.15470		6.9233
Ω_3^2	35.09216	33.77403	19.47019	18.16166		13.9777
Ω_4^2	54.79465	53.47580	30.64156	29.32637		22.8196
Ω_5^2	80.07961	78.75260	44.75928	43.43584		33.9295
Ω_6^2		107.47993		59.68744		46.7979
Ω_7^2		141.74693		78.86248		61.9154
Ω_8^2		179.50481		100.19542		78.8002
Ω_9^2		222.93466		124.52468		97.9907
Ω_{10}^2		267.27878		149.57948		117.824

frequency equations. In fact, the fundamental frequency of the semicircular arch ($\theta_0 = 180°$) as given by Archer (1960) agrees quite well with the DQM prediction. Other examples can be found in the literature (see Kang et al., 1996; Nelson, 1962);

- a comparison between the frequencies given by the approximate theory and the frequencies predicted by the exact theory shows that the errors grow with the deepness of the arch.

Moreover, the discrepancies seem to be larger than the relative errors given in Henrych (1981). Tables

Table 10
Shallow cantilever arches. Approximate theory

Ω^2	$\theta_0 = 20°$		$\theta_0 = 40°$		$\theta_0 = 80°$	
	Henrych	DQM	Henrych	DQM	Henrych	DQM
Ω_1^2	29.101	29.101	7.462	7.462	2.064	2.064
Ω_2^2	180.235	180.235	44.611	44.611	10.721	10.721
Ω_3^2	505.606	505.606	125.845	125.845	30.910	30.910
Ω_4^2	991.426	991.426	247.243	247.243	61.200	61.200
Ω_5^2	1639.392	1639.392	409.204	409.204	101.658	101.658
Ω_6^2	2449.366	2449.366	611.678	611.678	152.257	152.257
Ω_7^2	3421.348	3421.348	854.661	854.661	212.989	212.989
Ω_8^2	4555.335	4555.354	1138.147	1138.152	283.851	283.852
Ω_9^2	5851.325	5851.237	1462.137	1462.115	364.841	364.835
Ω_{10}^2	7309.317	7304.265	1826.630	1825.366	455.958	455.641

6–9 contain the first frequencies of the two-hinged arch, in the same order as described for the clamped case. The same conclusions can also be drawn.

Finally, the cantilever arch is examined in Tables 10–12. No comparison is made for the exact theory, because the higher frequencies are not reported elsewhere, and the fundamental frequency agrees completely with the exact eigenvalue.

If the opening angle θ_0 exceeds π, then, strictly speaking, we are not examining 'circular arches', but 'circular ring segments'. Nevertheless, the differential quadrature method can treat such systems without any significant difference.

As an example, the first five frequencies for some clamped, two-hinged and cantilever ring segments

Table 11
Deep cantilever arches. Approximate theory

Ω^2	$\theta_0 = 120°$		$\theta_0 = 160°$		$\theta_0 = 180°$
	Henrych	DQM	Henrych	DQM	DQM
Ω_1^2	1.084	1.084	0.766	0.766	0.6909
Ω_2^2	4.470	4.470	2.315	2.315	1.7489
Ω_3^2	13.337	13.337	7.197	7.197	5.5458
Ω_4^2	26.750	26.750	14.696	14.696	11.4455
Ω_5^2	44.707	44.707	24.775	24.775	19.3980
Ω_6^2	67.180	67.180	37.404	37.404	29.3694
Ω_7^2	94.161	94.161	52.572	52.572	41.3501
Ω_8^2	125.648	125.649	70.277	70.278	55.3366
Ω_9^2	161.638	161.635	90.517	90.516	71.3247
Ω_{10}^2	202.130	201.989	113.290	113.210	89.2544

Table 12
Cantilever arches. Exact theory

Ω^2	$\theta_0 = 20°$	$\theta_0 = 40°$	$\theta_0 = 80°$	$\theta_0 = 120°$	$\theta_0 = 160°$	$\theta_0 = 180°$
Ω_1^2	28.9274	7.2857	1.8763	0.87618	0.52815	0.435165
Ω_2^2	178.3529	42.8914	9.4711	3.66368	1.82747	1.37499
Ω_3^2	503.5454	123.9252	29.3702	12.13756	6.256133	4.70905
Ω_4^2	989.2592	245.2343	59.5971	25.48599	13.67251	10.5151
Ω_5^2	1637.1669	407.1414	100.0053	43.38528	23.68263	18.3922
Ω_6^2	2447.1050	609.5860	150.5844	65.83910	36.28622	28.3350
Ω_7^2	3419.0618	852.5459	211.2980	92.80177	51.43305	40.2922
Ω_8^2	4553.0487	1136.0221	282.1508	124.27967	69.127454	54.2662
Ω_9^2	5848.9259	1459.9801	363.1295	160.26047	89.357339	70.2453
Ω_{10}^2	7302.1479	1823.4022	454.0499	200.68549	112.09712	88.2107

Table 13
Ring sectors for clamped arches, two-hinged arches and cantilever arches

Ω^2		$\theta_0 = 240°$	$\theta_0 = 270°$	$\theta_0 = 330°$	$\theta_0 = 360°$
Ω_1^2	Clamped	1.98249	1.39493	0.74408	0.56642
	2-hinged	0.81792	0.47425	0.10129	6.3×10^{-9}
	Cantilever	0.28558	0.24743	0.20429	0.19244
Ω_2^2	Clamped	4.84947	3.58518	2.06358	1.59520
	2-hinged	3.30936	2.36576	1.24164	0.90074
	Cantilever	0.70139	0.54227	0.36571	0.31589
Ω_3^2	Clamped	9.32007	7.04140	4.26118	3.38459
	2-hinged	7.15772	5.34885	3.14174	2.44660
	Cantilever	2.25392	1.63160	0.91122	0.70006
Ω_4^2	Clamped	14.7627	11.3383	7.10834	5.75492
	2-hinged	12.1340	9.26743	5.72821	4.59667
	Cantilever	5.38323	4.02917	2.38964	1.87955
Ω_5^2	Clamped	21.5536	16.6663	10.6266	8.68973
	2-hinged	18.3264	14.1386	8.95660	7.29296
	Cantilever	9.73422	7.42214	4.58007	3.67660

are reported in Table 13. Some comparisons can be performed with the fundamental frequencies given in Kang et al. (1996), Archer (1960), Nelson (1962) for clamped and two-hinged arches, and the agreement is always noticeable.

The very small fundamental frequency of the simply supported complete ring should obviously be zero, but some unavoidable numerical approximation caused this negligible inaccuracy.

6. Conclusions

The dynamic analysis of circular arches in the presence of arbitrary constraints at the ends has been conducted by using a version of the differential quadrature method in which all the sixth boundary conditions can be satisfied exactly.

It is shown that the cantilever arch, where the eigenvalue appears also in the boundary conditions, can be studied without additional efforts.

Numerical examples and comparisons for arches and ring segments show that the DQM behaves very satisfactorily for every value of the opening angle, and a reduced number of Lagrangian coordinates allow the calculation of the higher frequencies.

Finally, it can be noted that the computational effort is greatly reduced by using a symbolic software (in our case, Mathematica), which also eliminated any numerical instability problems.

References

Archer, R.R., 1960. Small vibrations of thin incomplete circular rings. Int. J. Mech. Sci. 1, 45–56.

Auciello, N.M., De Rosa, M.A., 1994. Free vibrations of circular arches: a review. J. Sound Vibr. 176 (4), 433–458.

Bert, C.W., Malik, M., 1996. Differential quadrature method in computational mechanics: a review. Appl. Mech. Rev., ASME 49 (1), 1–28.

Chen, W., Striz, A.G., Bert, C.W., 1997. A new approach to the differential quadrature method for fourth-order equations. Int. J. Num. Meth. Engng 40, 1941–1956.

De Rosa, M.A., Franciosi, C., 1988a. On natural boundary conditions and DQM. Mech. Res. Comm. to appear.

De Rosa, M.A., Franciosi, C., 1998b. Nonclassical boundary conditions and DQM. J. Sound Vibr. 212 (4), 743–748.

Henrych, J., 1981. The Dynamics of Arches and Frames. Elsevier.

Kang, K.J., Bert, C.W., Striz, A.G., 1996. Vibration and buckling analysis of circular arches using DQM. Comp. and Struct. 60 (1), 49–57.

Nelson, F.C., 1962. In-plane vibrations of simply supported circular ring segment. Int. J. Mech. Sci. 4, 517–527.

Wang, X., Bert, C.W., Striz, A.G., 1993. Differential quadrature analysis of deflection, buckling, and free vibration of beams and rectangular plates. Comp. and Struct. 48, 473–479.

Wasserman, Y., 1977. The influence of the behaviour of the load on the frequencies and critical loads of arches with flexibly supported ends. J. Sound Vibr. 54 (4), 515–526.

Wolfram, S., 1991. Mathematica: A System for Doing Mathematics by Computer, 2nd ed. Addison-Wesley.